The Analysis of Synchronous All-to-All Communication Protocols for Wireless Systems

Haoliang Wang and Robert Simon
{hwang17,simon}@gmu.edu
George Mason University
Fairfax, Virginia, U.S.A

ABSTRACT

Many applications running over low-power and lossy wireless networks and wireless sensor networks (WSNs) rely heavily on a number of all-to-all communication primitives for services such as data aggregation, voting and consensus. Starting with the Chaos system, synchronous transmission-based broadcasting gossip protocols are now recognized as a technique for enabling efficient all-to-all communications in WSNs. However, despite their effectiveness, there has been relatively little analysis of this class of synchronous broadcasting gossip protocols (SBGPs). In this paper, we address this void by providing a basic theoretical framework for analysis SBGPs. Based on our derived theoretical results and previous experimental measurements, we show that the key for better performance is to increase the network connectivity as much as possible while limiting the number of concurrent transmitters. As a proof of the concept, we propose a multi-radio approach of the SBGP to achieve this purpose. We compare four multi-radio schemes of SBGP with a single radio SBGP through simulation and result has shown the convergence latency can be reduced up to 42% by utilizing multiple radios.

CCS CONCEPTS

• **Networks** → **Network performance modeling**; **Network simulations**; **Network performance analysis**; **Sensor networks**;

KEYWORDS

Synchronous Broadcasting Gossip Protocol; All-to-all Communication; Multi-Radio; Performance Modeling and Analysis

ACM Reference Format:
Haoliang Wang and Robert Simon. 2018. The Analysis of Synchronous All-to-All Communication Protocols for Wireless Systems . In *14th ACM International Symposium on QoS and Security for Wireless and Mobile Networks (Q2SWinet'18), October 28-November 2, 2018, Montreal, QC, Canada.* ACM, New York, NY, USA, 10 pages. https://doi.org/10.1145/3267129.3267134

1 INTRODUCTION

Protocols for efficient all-to-all message passing, data sharing, aggregation and distributed agreement are of high importance for the functioning of low-power wireless networks such as Wireless Sensor Networks (WSNs) [26]. Because of their simplicity and robustness, gossip-based protocols are among the most popular all-to-all communication techniques [20]. However, in WSN-like networks, where communication costs are the source of significantly high energy costs, conventional pairwise randomized and asynchronous gossip protocols suffer from poor speed and energy efficiency. Further, conventional gossip protocols typically do not take advantage of the broadcast nature of the wireless communications. As a result, there has been much interest recently in using synchronous-communication-based protocols to overcome these drawbacks and provide fast and efficient communication primitives.

One example is the Chaos system [16], where the capture effect and the flag-fields are utilized to achieve efficient all-to-all data aggregations. Experiments in Chaos have shown the effectiveness of such synchronous broadcasting gossip protocols (SBGPs). However, as its name suggests, communication patterns in protocols such as Chaos can be chaotic and non-trivial to analyze. Further, the actual performance of a typical SBGP remains unclear, limiting the ability of researchers to study fundamental operating characteristics such as convergence and latency. Therefore it is essential to provide theoretical result on the performance of SBGPs.

Though many theoretical results have been proposed [3, 6, 7, 9, 12, 13, 27], to our best knowledge, none of them are specifically derived based on the SBGP protocols. This paper addresses the above need by providing the basis of a theoretical model for SBGP protocols in low-power networks such as WSNs. We model synchronous communications in SBGP as a series of transformation of states, based on which, we have derived theoretical result on the convergence and its latency of SBGP. Several common network topologies in wireless networks are studied. The derived result for the convergence latency is exact for complete graphs and approximation for other types of topologies. We have validated the derived theoretical bound based on the numerical result, which shows the approximated result is accurate for various topologies.

With the theoretical result and the experiment results, we can then claim that, in order to improve the convergence latency and enable the SBGP to accommodate more dense and large wireless sensor networks, the key is to increase network connectivity and at the same time limit the number of concurrent transmitting nodes in the network. There are a few solutions proposed previously to address these issues with multiple channel approaches [1, 2, 22]. In this paper, we take a different angle and investigate a new multi-radio approach to improve the convergence latency of SBGPs. With advancement in communication technologies, wireless sensor nodes that concurrently support multiple radios with different frequencies and capabilities on a single platform become widely available, e.g.

Q2SWinet'18, October 28-November 2, 2018, Montreal, QC, Canada

ACM ISBN 978-1-4503-5963-4/18/10…$15.00
https://doi.org/10.1145/3267129.3267134

Zolertia RE-Mote. More and more systems start to adopt such multi-radio nodes as a way to improve performance. As for the SBGP, multiple radios provide a good solution to increase the network connectivity without increasing the probability of interference to the capture effect in large and dense networks.

Hence in this paper, we continue to investigate how to adopt multi-radio in SBGP so that the potential of multiple heterogeneous radios can be fully exploited to accelerate the dissemination of information. To this end, we introduce a hierarchy into the network by dividing the network into multiple clusters of two or more levels. As a proof of concept, we propose four multi-radio-based SBGP schemes with different inter/intra-cluster protocols and temporal orders. The proposed four multi-radio schemes are evaluated through simulations in MASON simulation toolkit with different scenarios. Result showed that the multi-radio approach is able to reduce the convergence latency up to 42% compared with the single radio SBGP. Among the four schemes, the many-to-many simultaneous scheme performs the best overall while the many-to-many sequential scheme performs slightly worse but may potentially save significantly more energy. The many-to-one schemes also show its performance advantages in case of small cluster size.

To summarize, the contribution of our paper is three-fold:

- We bridged the gap of the modeling and analysis of the convergence and latency of SBGP. Case studies are provided for common network topologies and result are verified through numerical calculations and simulations, providing guidance for SBGP-related performance analysis and improvements;
- We proposed and studied novel multi-radio-based approaches to achieve better all-to-all communication latency performance with SBGP;
- We investigated and evaluated various configurations through simulation and identified the scenarios where each of the four multi-radio schemes performs well.

The rest of this paper is organized as follows: in Section 2 we will provide background information for the SBGP for all-to-all communications and the Chaos system. In Section 3, we provide performance models and convergence results of the SBGP. In Sections 4, we introduce the approach to adopt multi-radio into SBGP for better scalability. We evaluated the proposed four schemes and compared them with the single radio SBGP in Section 5. We will conclude this paper in Section 6.

2 BACKGROUND AND RELATED WORK

For wireless networks, broadcasting gossip protocols are long been proposed to utilize the broadcasting nature of wireless communication so that each node can send its information to multiple neighbors at a time [7]. For many of these protocols, communications is asynchronous — nodes wake up independently and transmit the packets in a CSMA fashion. To further improve the efficiency and latency of the all-to-all communications, *Synchronous Broadcasting Gossip Protocols* (SBGP) are proposed, where each node wakes up synchronously and either transmit packets and receive packets from others at the same time. When two nodes transmit at the same time, we usually consider it as a collision and the receiver will not get anything from either node. In reality, with certain conditions [18], the receiver can demodulate only one signal and completely suppress all others, therefore receiving from one of the senders despite the collision. Such phenomenon is called the *Capture Effect*. SBGPs take the advantage of *Capture Effect* for nodes to communicate. In case of multiple concurrent transmitters, because of Capture Effect, a receiver still has the chance to receive from one of the transmitters. Even though the *Packet Reception Ratio* (PRR) per transmission may decrease due to interference comparing to the asynchronous protocols, the synchronous protocol eliminates some of the transmission overhead (e.g. preambles and collision detections) so that during the same time period nodes can perform many more rounds of synchronous transmissions, reducing the overall latency and increasing the efficiency, as demonstrated by many previous works [1, 2, 10, 16, 22].

The Chaos system, introduced by Landsiedel, et al. [16] is one of the first examples of SBGP for all-to-all communications in the wireless domain. Chaos is explicitly designed for data aggregation among all the nodes in WSNs. In Chaos, the packet is designed to consist two parts: flags and payload. The flags are bit array indicating which node has participated in generating the payload. The flag array is used to help accelerate the aggregation process compared with the conventional mixing. With the flag field, the user will have the opportunity to define a merge function which will be used to aggregate the node's own data with the payload when receiving a new packet. When all flags are set, the payload is the final result and will be delivered to the application. Based on this simple strategy, performance can be poor when too many nodes are trying to transmit simultaneously. The authors proposed a propagation policy that the node only transmits when it receives new information from other nodes so that some transmissions can be suppressed to avoid too many contentions.

Due to the properties of the capture effect, performance issues persist in large scale networks for Chaos. Other follow-up works have been proposed to address some of the scalability issues. In [22], the Chaos system and its primitives are ported to Bluetooth Low Energy platforms. Experiments show that the performance is not as good as is in the original Chaos systems with 802.15.4 radio and the authors argue that the primary reason is the channel interference. To improve the performance and mitigate channel interference, a multi-channel approach is proposed. Extreme Chaos [10], a new coordinating data structure based on order-statistics theory is proposed to replace the flag field so that the system can estimate the aggregation result with less accuracy but higher scalability and tolerance with network dynamics. Evaluation showed the aggregation latency of Extreme Chaos was reduced up to 15% with comparable reliability. In [2], the authors argue that the original Chaos design is only robust in low and medium level of interference. Once channels become jammed for a long duration, i.e., more than a couple of milliseconds, the reliability in Chaos drops and latency and energy consumption increases. Multiple channel and channel hopping techniques are used to mitigate the interference. Besides, local and global channel blacklisting is implemented to avoid channels with high interference.

Despite the effectiveness demonstrated in SBGPs for all-to-all communications, the theoretical performance modeling and analysis of the SBGP protocols, which is valuable for designing and analyzing networks and protocols, is not well-studied. The communication and information exchange patterns in SBGP differ significantly

from other previously studied gossip-based protocols. For example, in [7], a simple asynchronous model is studied where nodes wake up independently and choose only one neighbor in random to exchange information in a symmetric way. In [3], the broadcast nature of wireless communications is considered and utilized in the proposed model to exchange information in asymmetric way. However, at each time step, still only one node can asynchronously wake up and broadcast its information to its neighbors. In [12], a synchronous unicast gossip-based protocol is studied. However, neither the broadcast nature of wireless communication nor half-duplex radio transmission limitation are properly considered in the model. Currently to our best knowledge, no performance model and analysis result has been derived specifically for SBGP.

3 CONVERGENCE AND LATENCY ANALYSIS

In this section, we will first introduce our model of the SBGP protocol and provide the result on its convergence and the latency. We will study several common network topologies and provide theoretical bounds on convergence latency. Finally we will briefly validate the theoretical result through numerical result and simulations.

3.1 Model

3.1.1 Basic Notations. We model the wireless network as a static undirected graph G where there is an edge in G if the two nodes are within the communication range of the radio. The total number of nodes is N and each node is numbered from $[1, ..., N]$. The set of neighbors of node i is represented as N_i. The adjacency matrix of G is denoted as $\boldsymbol{A}$, where $\boldsymbol{A}_{ij} = 1$ if and only if there is an edge connecting node i and j. The degree matrix is denoted as $\boldsymbol{D}$, where $\boldsymbol{D}_{ii} = |N_i|$. The *Laplacian* matrix of the graph is therefore $\boldsymbol{L} = \boldsymbol{D} - \boldsymbol{A}$. The ith eigenvalue of a square matrix $\boldsymbol{A}$ of dimension N is denoted as $\lambda_i(\boldsymbol{A})$ and we sort the eigenvalues so that $\lambda_1(\boldsymbol{A}) \geq \lambda_2(\boldsymbol{A}) \geq ... \geq \lambda_N(\boldsymbol{A})$. $\lambda_{N-1}(\boldsymbol{L})$ is called the *algebraic connectivity* of the graph [14] and will be shown later as an important parameter in determining the convergence of the protocol. $\boldsymbol{I}$ is the identity matrix and $\boldsymbol{J}$ is a all-one matrix divided by its dimension $\boldsymbol{J} = \vec{1} \cdot \vec{1}^T / N$. The following Table 1 summarizes the notations used in the modeling and analysis of this paper.

3.1.2 Wireless Communication. In the synchronous communication scenario, the time is divided into slots and at every time slot t, all the nodes communicate simultaneously. At each time slot, a node may choose to broadcast its message or choose to listen. If the node chooses to listen, because of the *Capture Effect*, it will either successfully receive the message from one of its neighbors that are broadcasting, or receive nothing due to interferences (we treat such case as if the node receives the value from itself). If the node chooses to broadcast, it will not able to receive anything due to the half-duplex nature of the radio, and therefore, the broadcasting node will also be treated as if it receives the value from itself. We denote all the nodes' choice at the time slot t as a vector $\vec{j}(t)$ with its ith component defined as follows,

$$\vec{j}_i(t) = \begin{cases} i & \text{if node } i \text{ broadcasts} \\ i & \text{if node } i \text{ receives nothing} \\ k & \text{if node } i \text{ receives from node } k \in N_i \end{cases} \quad (1)$$

Table 1: List of Notations

Symbol	Description
G	Network graph
$\boldsymbol{A}$	Adjacency matrix of the graph
$\boldsymbol{D}$	Degree matrix of the graph
$\boldsymbol{L}$	Laplacian matrix of the graph
$\boldsymbol{I}$	Identify matrix
$\boldsymbol{J}$	All-one matrix divided by its dimension
$\lambda_i(\boldsymbol{A})$	ith largest eigenvalue of a matrix $\boldsymbol{A}$
$\vec{j}(t)$	Transmission vector defined in Eq. 1
C_G	Number of all viable $\vec{j}$ for graph G
$\boldsymbol{R}_G$	A matrix where $\boldsymbol{R}_G^{ij}$ represents the number of $\vec{j}$ where node i receives from node j for graph G
$\boldsymbol{S}_G$	A matrix where $\boldsymbol{S}_G^{ij}$ represents the number of $\vec{j}$ where node i is received by j nodes for graph G
α	Mixing parameter
$x_i(t)$	The value of node i at time step t
$\boldsymbol{W}_{\vec{j}(t)}$	State transformation matrix defined in Eq. 3
N	Total number of nodes
N_i	The set of neighbors of node i
$T(N, \epsilon)$	ϵ-converging time
$\mathscr{K}_N$	Complete graph with N nodes
$\mathscr{O}_N$	Ring graph with N nodes
$\mathscr{R}_{N,d}$	d-regular graph with N nodes
$\mathscr{G}_N$	Geometric random graph with N nodes

Hence, every $\vec{j}(t)$ is a combination of those choices with its ith component chosen from the set $\{i\} \cup N_i$. In other words, $\vec{j}$ depicts the information exchange between nodes in one time slot. Note that not all combinations in $\vec{j}$ are viable because a node can only receive from another node that is broadcasting. Such *Half-duplex* constraints are represented as follows,

$$\vec{j}_{\vec{j}_i} = \vec{j}_i, \ \forall i \in [1, ..., N]$$

In other words, if a node i receives from node $\vec{j}_i$, the node $\vec{j}_i$ must be broadcasting and therefore, receive from itself.

The probability that a certain $\vec{j}$ is chosen varies based on the specific protocol design (e.g., transmission in some time slots may be suppressed for certain nodes to save energy or reduce collisions) and the environment conditions, which are difficult to model. Here for simplicity, in our analysis, we assume the sequence of $\vec{j}(t)$ that is chosen by the nodes is *Independent and Identically Distributed (i.i.d.)*. Hence we have the following,

$$Prob\{\vec{j} = \vec{j}(t)\} = \frac{1}{C_G} \quad (2)$$

where C_G represents the number of all viable combinations of $\vec{j}$ for the specific graph G. We also have a matrix $\boldsymbol{R}_G$, where R_G^{ij} represents the number of combinations that a node i receives messages from its neighbor node j. Clearly, $R_G^{ij} = 0$ if $A_{ij} = 0$. The rest of the values in $\boldsymbol{R}_G$, however, depend on the specific graph topology. We also have another matrix $\boldsymbol{S}_G$, where S_G^{ij} represents the number of combinations that a total of j nodes successfully receive the message broadcast from node i. Similar to $\boldsymbol{R}_G$, the values in $\boldsymbol{S}_G$ depend on the graph topology. Note that if the graph G is symmetric, $\boldsymbol{R}_G$ will

degenerate into a scalar, represented as R_G while $\boldsymbol{S}_G$ will degenerate into a vector, represented as $\vec{S}_G$. We will study the properties of C_G, $\boldsymbol{R}_G$, and $\boldsymbol{S}_G$ later in this paper.

3.1.3 Gossip-based Protocol. There are many ways for the gossip-based protocols to handle the incoming information from other nodes in order to achieve various objectives such as data aggregation or consensus. Here, as an example of our analysis, we choose a common mixing approach to calculate the network-wide average. In this data mixing scheme, each node has its initial value and the goal is to reach a consensus on the average of all nodes' values through gossiping. During time slot t where node i receives the value from node j, node i updates its own value according to the following mixing process,

$$x_i(t+1) = (1-\alpha)\cdot x_i(t) + \alpha \cdot x_j(t)$$

where $x_i(t)$ represents the value of node i at time t and α is a constant mixing parameter. Based on a similar modeling technique used in previous works [3, 7, 12], we can then write the state transformation for all the nodes from time t to time $t+1$ as the following matrix multiplication,

$$\vec{x}(t+1) = \boldsymbol{W}_{\vec{j}(t)} \cdot \vec{x}(t)$$

where the element of $\boldsymbol{W}_{\vec{j}(t)}$ is given by,

$$\boldsymbol{W}^{ik}_{\vec{j}(t)} = \begin{cases} 1 & \text{if } k = i \text{ and } k = \vec{j}_i(t) \\ (1-\alpha) & \text{if } k = i \text{ and } k \neq \vec{j}_i(t) \\ \alpha & \text{if } k \neq i \text{ and } k = \vec{j}_i(t) \\ 0 & \text{otherwise} \end{cases} \tag{3}$$

We can then get the expected state transformation matrix $\overline{\boldsymbol{W}}$ based on Eq. 2 as follows,

$$\overline{\boldsymbol{W}} = \sum_{\vec{j}} Prob\{\vec{j}\}\boldsymbol{W}_{\vec{j}} = \boldsymbol{I} - \frac{\alpha}{C_G} diag\{\boldsymbol{R_G}\cdot\vec{1}\} + \frac{\alpha}{C_G}\boldsymbol{R_G}$$

Clearly, all $\boldsymbol{W}_{\vec{j}(t)}$ and $\overline{\boldsymbol{W}}$ are right-stochastic matrices but not left-stochastic, which indicates that the SBGP is asymmetric and may result in a network-wide consensus but the consensus value will not be the average of the initial values [7]. We will study the protocol's convergence and its latency in the following subsections.

3.2 Convergence

Here we want to show that the SBGP converges to a network-wide consensus (not necessarily the average of nodes' initial values) almost surely.

Proposition 3.1. The synchronous broadcasting gossip protocol converges to a consensus value c with probability 1, which is

$$Prob\{\lim_{t\to\infty}\vec{x}(t) = c\vec{1}\} = 1 \tag{4}$$

where the expectation of c is the average of the nodes' initial values $E(c) = \frac{1}{N}\vec{1}^T\vec{x}(0)$.

Proof The information exchange ($\vec{j}(t)$) in a single time slot in the SBGP studied in this paper can be divided into at most n separate steps, where in each such *sub-time-slot*, only one node will broadcast to a subset of its neighbors. Therefore, the convergences of the synchronous protocol is equivalent to that of the asynchronous protocol defined in [3]. As shown in the Theorem.1 in [3], the asynchronous broadcasting gossip protocol has been proven to converge to a consensus almost surely and hence, the synchronous protocol converges to a consensus almost surely as well. Given the fact that $\boldsymbol{W}_{\vec{j}(t)}$ is a right-stochastic matrix, the mathematical proof of the convergence of the synchronous protocol is in fact the same with the asynchronous protocol and therefore omitted here. □

3.3 Convergence Latency

Next we are interested in the latency or the rate of the convergence of the SBGP. Here we use the notion of ϵ-converging time defined in [3, 7] as the metric of the convergence latency.

Definition 3.1. The ϵ-converging time is the earliest time slot k when the vector $\vec{x}(k)$ is *ϵ-close* to the normalized initial deviation with probability greater than $1-\epsilon$:

$$T(N,\epsilon) = \sup_{\vec{x}(0)}\left\{inf\left\{k : Prob\left\{\frac{\left\|\vec{x}(k) - \boldsymbol{J}\cdot\vec{x}(k)\right\|_2}{\left\|\vec{x}(0) - \boldsymbol{J}\cdot\vec{x}(0)\right\|_2} \geq \epsilon\right\} \leq \epsilon\right\}\right\}$$

Based on the result in [7], $T(N,\epsilon)$ can be bounded as follows,

$$\frac{0.5\cdot log\epsilon^{-1}}{log(\lambda^{*-1})} \leq T(N,\epsilon) \leq \frac{3\cdot log\epsilon^{-1}}{log(\lambda^{*-1})} \tag{5}$$

where $\lambda^* = \lambda_1 E\{\boldsymbol{W}^T\cdot(\boldsymbol{I}-\boldsymbol{J})\cdot\boldsymbol{W}\}$ is the largest eigenvalue of the expectation of $\boldsymbol{W}^T_{\vec{j}}\cdot(\boldsymbol{I}-\boldsymbol{J})\cdot\boldsymbol{W}_{\vec{j}}$ over all possible $\vec{j}$s. It is the key to determine the bound of the convergence latency.

As we will show shortly, the closed-form expression of the above expectation and λ^* are too complicated to obtain without any prior knowledge of the underlying network graph. Hence, for our analysis in this paper, we first assume a complete network graph and use the result of the complete graph to obtain approximated result for other general topologies.

Proposition 3.2. The largest eigenvalue of the expectation of $\boldsymbol{W}^T_{\vec{j}}\cdot(\boldsymbol{I}-\boldsymbol{J})\cdot\boldsymbol{W}_{\vec{j}}$ can be approximated as follows,

$$\lambda^* \simeq 1 - 2\alpha(1-\alpha)\frac{R_G}{C_G}\lambda_{N-1}(\boldsymbol{L}) - \alpha^2\frac{\hat{S}_G + R_G}{NC_G}\lambda_{N-1}(\boldsymbol{L}) \tag{6}$$

where $\hat{S}_G = \frac{1}{|N_i|}\sum_{i=1}^{|N_i|}(i^2\vec{S}^i_G)$. The approximation becomes exact when G is complete graph of size N.

Proof First we denote $\boldsymbol{W}'_{\vec{j}} = \boldsymbol{W}^T_{\vec{j}}\cdot\boldsymbol{W}_{\vec{j}}$ and $\boldsymbol{W}''_{\vec{j}} = \boldsymbol{W}^T_{\vec{j}}\cdot\boldsymbol{J}\cdot\boldsymbol{W}_{\vec{j}}$. Then we have,

$$E\{\boldsymbol{W}^T_{\vec{j}}\cdot(\boldsymbol{I}-\boldsymbol{J})\cdot\boldsymbol{W}_{\vec{j}}\} = E\{\boldsymbol{W}'_{\vec{j}}\} - E\{\boldsymbol{W}''_{\vec{j}}\}$$

Based on our definition of $\boldsymbol{W}_{\vec{j}}$ in Eq.3, for $\boldsymbol{W}'_{\vec{j}}$, we have,

$$\begin{aligned}\boldsymbol{W}'^{ij}_{\vec{j}} &= \sum_{k=1}^{n}\boldsymbol{W}^{ki}_{\vec{j}}\boldsymbol{W}^{kj}_{\vec{j}} \\ &= \begin{cases} 1 + d^i(\vec{j})\alpha^2 & \text{if } i = j \text{ and } j = \vec{j}_i \\ (1-\alpha)^2 & \text{if } i = j \text{ and } j \neq \vec{j}_i \\ (1-\alpha)\alpha & \text{if } i \neq j \text{ and } (j = \vec{j}_i \text{ or } i = \vec{j}_j) \\ 0 & \text{otherwise} \end{cases}\end{aligned} \tag{7}$$

For $\boldsymbol{W}''_{\vec{j}}$, we have,

$$\boldsymbol{W}''_{\vec{j}} = \frac{1}{N} \cdot (\mathbf{1}^T \cdot \boldsymbol{W}_{\vec{j}})^T \cdot (\mathbf{1}^T \cdot \boldsymbol{W}_{\vec{j}}) = \frac{1}{N} \begin{cases} (1 + d^i(\vec{j})\alpha)^2 & \text{if } i = j, j = \vec{j}_i \\ (1-\alpha)^2 & \text{if } i = j, j \neq \vec{j}_i \\ (1 + d^i(\vec{j})\alpha)(1 + d^i(\vec{j})\alpha) & \text{if } i \neq j, i = \vec{j}_i, j = \vec{j}_j \\ (1 + d^i(\vec{j})\alpha)(1-\alpha) & \text{if } i \neq j, i = \vec{j}_i, j \neq \vec{j}_j \\ (1 + d^j(\vec{j})\alpha)(1-\alpha) & \text{if } i \neq j, i \neq \vec{j}_i, j = \vec{j}_j \\ (1-\alpha)^2 & \text{if } i \neq j, i \neq \vec{j}_i, j \neq \vec{j}_j \end{cases} \tag{8}$$

The $d^i(\vec{j})$ in Eq. 7 and 8 represents the number of destinations that node i sends its packet to based on that specific $\vec{j}$ and it satisfies $0 \leq d^i(\vec{j}) \leq |N_i|, \forall \vec{j}$.

Without any prior knowledge of the graph, the closed-form expression of $E\{\boldsymbol{W}' - \boldsymbol{W}''\}$ is non-trivial to obtain because it is hard to find the number of cases that two nodes are received by some other nodes simultaneously (Case 3 through 6 in Eq. 8). Fortunately, if we assume the underlying graph is a complete graph, we can easily obtain the expression for both $E\{\boldsymbol{W}'\}$ and $E\{\boldsymbol{W}''\}$ as follows,

$$E\{\boldsymbol{W}'\} = \boldsymbol{I} - 2\alpha(1-\alpha)\frac{R_G}{C_G}\boldsymbol{L}\,,\ E\{\boldsymbol{W}''\} = \boldsymbol{J} + \alpha^2\frac{\hat{S}_G + R_G}{N \cdot C_G}\boldsymbol{L}$$

With a similar argument as Appendix G in [3], the λ^* can then be obtained as follows,

$$\begin{aligned} \lambda^* &= \lambda_1(E\{\boldsymbol{W}' - \boldsymbol{W}''\}) \\ &= 1 - 2\alpha(1-\alpha)\frac{R_G}{C_G}\lambda_{N-1}(\boldsymbol{L}) - \alpha^2\frac{\hat{S}_G + R_G}{NC_G}\lambda_{N-1}(\boldsymbol{L}) \end{aligned} \tag{9}$$

The above result holds for complete graph and can be used to approximate the result of other graphs. □

Corollary 3.1. The ϵ-Converging Time of the synchronous broadcasting gossip protocol in a complete graph of size N is asymptotically bounded as follows,

$$T(N, \epsilon) = \Theta\Big(\frac{log\epsilon^{-1}}{\alpha(1-\alpha)N\frac{R_G}{C_G} + \alpha^2\frac{\hat{S}_G + R_G}{C_G}}\Big) \tag{10}$$

Proof The second largest eigenvalue of the graph Laplacian L for the complete graph is always N. Using Eq.4 and taking the approximation of $log(x^{-1}) \simeq 1 - x$, the above equation can be immediately obtained. □

3.4 Case Analysis

In this subsection, based on Proposition 3.2, we will study the value of C_G, R_G, and $\vec{S}_G$ in different types of graphs. As aforementioned, the result shown in the Proposition 3.2 applies only to complete graphs. However, with different topology-specific C_G, R_G and $\hat{S}_G$, we may be able to approximate the latency result for other graph topologies based on Proposition 3.2. For the rest of this subsection, we will count the C_G, R_G and $\hat{S}_G$ of the complete topology, ring topology and other d-regular topologies and compare the approximated result against the numerically generated result. In all the numerical result, we fix the mixing parameter $\alpha = 0.5$.

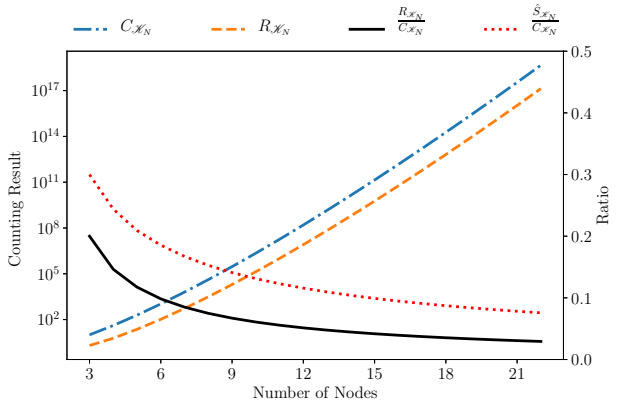

Figure 1: $C_{\mathscr{K}_N}$, $R_{\mathscr{K}_N}$, and their ratios with $N \in [2, 21]$

3.4.1 Complete Graph. Now we study the values of C_G, R_G, and $\vec{S}_G$ when G a complete graph of size N, denoted $G = \mathscr{K}_N$. To this end, we first need to count the number of all viable combinations of $\vec{j}$. Such counting problem for a complete graph $\mathscr{K}_N$ is equivalent to the following problem [23]: "*Count the number of idempotent self-mappings in a N-element set.*" The result can be derived as the following summations:

$$C_{\mathscr{K}_N} = \sum_{k=0}^{N}\binom{N}{k}\cdot(N-k)^k \quad , \quad R_{\mathscr{K}_N} = \sum_{k=1}^{N-1}\binom{N-2}{k-1}\cdot k^{(N-1-k)}$$

For $\vec{S}_{\mathscr{K}_N}$, the counting problem for the ith component in $\vec{S}_{\mathscr{K}_N}$ is equivalent to the following problem [17, 24]: "*Count the number of partial idempotent mappings with breadth exactly $N - i$.*" The result is given by the following summation:

$$\vec{S}^i_{\mathscr{K}_N} = \binom{N}{i}\sum_{k=0}^{N-i}\binom{N-i}{k}\cdot k^{N-i-k}$$

Hence,

$$\begin{aligned} \hat{S}_{\mathscr{K}_N} &= \frac{\sum_{i=1}^{N-1}\Big(i^2\binom{N}{i}\sum_{k=0}^{N-i}\binom{N-i}{k}\cdot k^{N-i-k}\Big)}{N-1} \\ &= \sum_{k=0}^{N-1}\binom{N-1}{k}\cdot(N-k-1)^k = C_{\mathscr{K}_{N-1}} \end{aligned}$$

Figure 1 shows the result for $C_{\mathscr{K}_N}$, $R_{\mathscr{K}_N}$, $\frac{\hat{S}_{\mathscr{K}_n}}{C_{\mathscr{K}_N}}$ and $\frac{R_{\mathscr{K}_N}}{C_{\mathscr{K}_N}}$, with $N \in [2, 21]$. Clearly, the ratio of both $R_{\mathscr{K}_N}$ and $\hat{S}_{\mathscr{K}_N}$ over $C_{\mathscr{K}_N}$ decreases with the increase of the number of nodes. Specifically, from the graph we can see both ratios can be asymptotically bounded by $\Omega(N^{-1})$. Hence, we can immediately obtain the following corollary:

Corollary 3.2. If we let $\epsilon = N^{-\alpha}$, the ϵ-convergence latency for the complete graph $\mathscr{K}_N$ is,

$$T(N, N^{-\alpha}) = O(logN) \tag{11}$$

Since up to N transmissions could happen at each time step, the communication complexity is therefore $O(N \cdot logN)$. Since every node is able to communicate with any other node in the network in a complete topology, the above result matches the bound derived for conventional push-based gossip protocol in wired networks.

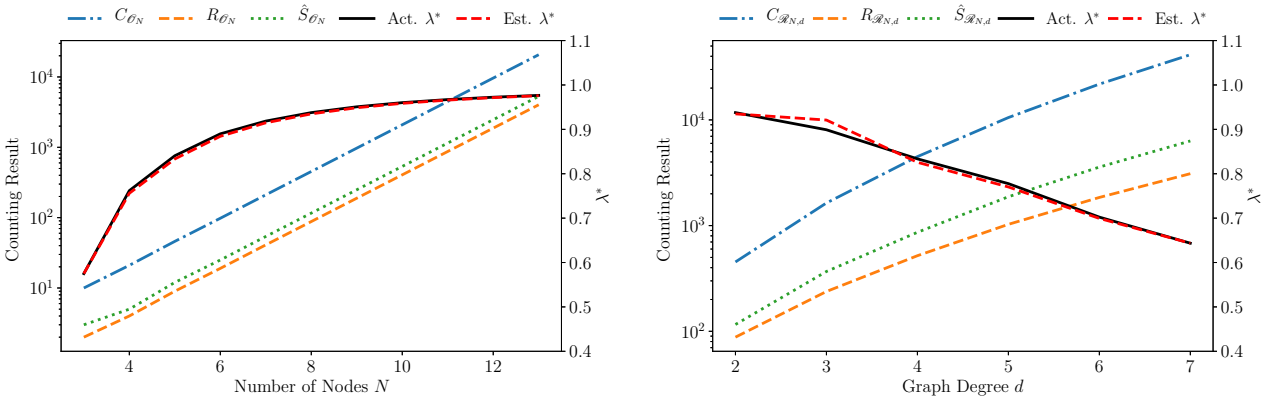

(a) Ring Graph $\mathscr{O}_N$ **(b) d-Regular Graph $\mathscr{R}_{N,d}$**

Figure 2: Counting Result for C_G, R_G, and $\hat{S}_G$ (left y-axis) and actual and estimated λ^* (right y-axis) for various topologies

3.4.2 Ring Graph. Similar to the case of complete graph, the counting problem for C_G, R_G and $\hat{S}_G$ for the ring topology (denoted as $\mathscr{O}_N$) can be reduced to the following problem [25]: "*Count the number of independent vertex sets in d-antiprism graph.*" The result is given by the following linear recurrence relation $X_n(a,b,c)$ and (a,b,c) is the set of the initial three values.

$$X_n = X_{n-1} + 2X_{n-2} + X_{n-3}, \forall n \geq 3$$

$C_{\mathscr{O}_N}$, $R_{\mathscr{O}_N}$ and $\hat{S}_{\mathscr{O}_N}$ are determined by the same recurrence but with different sets of initial values. Specifically,

$$C_{\mathscr{O}_N} = X_n(3,1,5),\ R_{\mathscr{O}_N} = X_n(1,0,1),\ \hat{S}_{\mathscr{O}_N} = X_n(2,0,1) \quad (12)$$

The second smallest eigenvalue of the Laplaician matrix of the $\mathscr{O}_N$ graph is known to be the following,

$$\lambda_{N-1}(\boldsymbol{L}_{\mathscr{O}_N}) = 2(1 - cos(\frac{2\pi}{N})) \simeq \frac{4\pi^2}{N^2} \quad (13)$$

where the last approximation holds when N is significantly greater than 2π. With Eq. 12 and Eq. 13, we can now calculate the approximated λ^* for $\mathscr{O}_N$ graph. For the actual λ^*, we obtain it by enumerating all possible $\vec{j}$ in the $\mathscr{O}_N$ graph and its corresponding $\boldsymbol{W}_{\vec{j}}$ and numerically calculating of the largest eigenvalue of the expected matrix. Here we choose $\alpha = 0.5$. Figure 2a shows the counting result and the actual and approximated value for λ^* for $\mathscr{O}_N$ with $N \in [2, 21]$. First we can observe from the counting result that all three values increases exponentially however the ratios between them, specifically, $R_{\mathscr{O}_N}/C_{\mathscr{O}_N}$ and $\hat{S}_{\mathscr{O}_N}/C_{\mathscr{O}_N}$, converge to an constant ($\simeq 0.1943$ and 0.2559, respectively) as the size of the ring graph increases. In other words, $R_{\mathscr{O}_N}/C_{\mathscr{O}_N} = \hat{S}_{\mathscr{O}_N}/C_{\mathscr{O}_N} = \Theta(1)$. Next, we compare the two λ^*. From the figure, we can clearly see that the approximated value is very close to the actual value, which indicates a good approximation of λ^* and subsequently a good estimate of $T(N,\epsilon)$, which then can be immediately derived as the following corollary,

Corollary 3.3. If we let $\epsilon = N^{-\alpha}$, the ϵ-convergence latency for the ring graph $\mathscr{O}_N$ is,

$$T(N, N^{-\alpha}) = O(N^2 \cdot logN) \quad (14)$$

3.4.3 Regular Graph. To study impact of the density of a graph to the convergence latency of the synchronous communication., we consider a more general d-regular topology, denoted as $\mathscr{R}_{N,d}$. With solely the knowledge of a d-regular topology, it is not possible to derive the exact expression for $C_{\mathscr{R}_{N,d}}$, $R_{\mathscr{R}_{N,d}}$ and $\hat{S}_{\mathscr{R}_{N,d}}$, as well as its algebraic connectivity ($\lambda_{N-1}(\boldsymbol{L}_{\mathscr{R}_{N,d}})$). Therefore, to examine the accuracy of the approximation in Eq. 9, we numerically calculate the value of $C_{\mathscr{R}_{N,d}}$, $R_{\mathscr{R}_{N,d}}$ and $\hat{S}_{\mathscr{R}_{N,d}}$. Also, we use the actual value of $\lambda_{N-1}(\boldsymbol{L}_{\mathscr{R}_{N,d}})$ of the randomly generated regular graph, along with asymptotic bounds. The result of a 8-node d-regular graph with $d \in [2, 7]$ is shown in Figure 2b.

As we can see from the figure, the counting result of all three values increases exponentially and the ratios $R_{\mathscr{R}_{N,d}}/C_{\mathscr{R}_{N,d}}$ and $\hat{S}_{\mathscr{R}_{N,d}}/C_{\mathscr{R}_{N,d}}$ decreases as the degree increases. Specifically, we may obtain from the figure that,

$$\frac{R_{\mathscr{R}_{N,d}}}{C_{\mathscr{R}_{N,d}}} = \frac{\hat{S}_{\mathscr{R}_{N,d}}}{C_{\mathscr{R}_{N,d}}} = \Theta(\frac{1}{d})$$

Meanwhile, the approximation of λ_1 remains very close to the actual value with relatively more variation when the network is sparse and converges to the actual value when the network becomes increasingly denser, indicating our approximation of λ^* remains reasonably accurate for regular graphs with different degrees. Hence, approximation in Eq. 9 is accurate and with proper result on the algebraic connectivity of the regular graphs, one can easily obtain the performance bounds of the SBGP under various topologies. Since the study of the algebraic connectivity is out of the scope, we do not pursue such bounds in this paper.

3.5 Validation

With all the theoretical result derived, we now validate the result through simulation. We implemented the SBGP in MASON multi-agent simulator [19] (more details regarding the implementation will be provided later in Section 5). Since the capture effect is not considered in our model (which affects the reception rate based on the number of concurrent transmitters), we will generate the simulation result with and without capture effect implemented in the simulation and compare them against the theoretical result (we

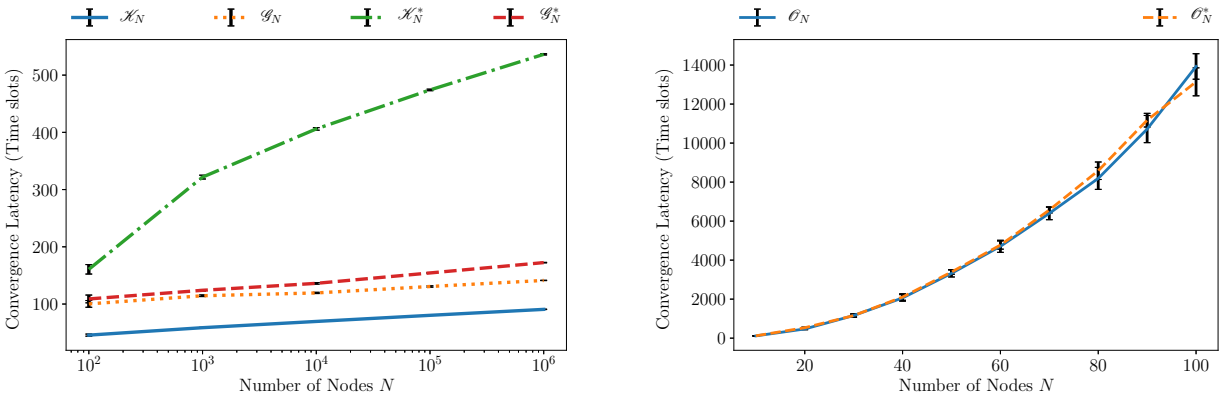

(a) Complete Graph $\mathscr{K}_N$ and Geometric Random Graph $\mathscr{G}_N$ **(b) Ring Graph $\mathscr{O}_N$**

Figure 3: Simulated Convergence Latency for Various Topologies (* means capture effect is modeled in the simulation)

use capture effect measurements from [16]). Figure 3a and 3b show the simulation result for complete graph $\mathscr{K}_N$ and geometric random graph $\mathscr{G}_N$ which can seen in expectation as a $\Theta(logN)$-regular graph, and the ring graph $\mathscr{O}_N$. The * in the figures indicates the result is obtained with capture effect considered. First, from the simulation result without the effect from the concurrent transmitters considered, we can see from the figures that the $\mathscr{K}_N$ and $\mathscr{O}_N$ result match the theoretical result. Also the $\mathscr{G}_N$ result is above the lower bound (complete graph). Hence, with the case studies and the numerical result, we are confident that our result in Proposition 3.2, though derived with the assumption of a complete graph, can be used to actually approximate the result of other type of graphs. With the result on the the complete graph and the ring graph, we have essentially provided a lower and upper bound for graphs with degrees within $[2, N-1]$.

When taking the effect from the concurrent transmitters into the consideration, $\mathscr{O}_N^*$ remains unaffected because any node can only experience two concurrent transmitters due to the degree where the reception rate under two transmitters is still above 60%. For $\mathscr{K}_N^*$ and $\mathscr{G}_N^*$, individually both of them match the asymptotic bounds derived for their corresponding topology, indicating a good asymptotic tightness. However, if we compare the result of $\mathscr{K}_N^*$ and $\mathscr{G}_N^*$, we find that the SBGP in the complete graph performs much worse compared with the geometric random graph, deviating from the theoretical result. Such simulation result matches the experience in real world — with the same network and higher transmission range, the convergence latency of SBGP usually does not monotonically decrease. This is because the success rate of receiving packet through capture effect decreases dramatically with increasing probabilities of high concurrent transmitters, as observed in various experimental results [16, 18]. Our proposed performance analysis does not model the success rate of capture effect with regard to the number of concurrent transmissions. Therefore, even though a high connectivity enables the message to be sent to far away node which accelerates the convergence, the lower successful reception rate due to high interference counteracts the such advantage and may eventually lead to worse performance. In the next section, we will discuss new approaches to utilize both seemingly contradicting theoretical and experimental result for better performance of SBGP.

4 MULTI-RADIO APPROACH

As shown in previous section, on the one hand, the performance model tells us that in order to obtain better convergence latency, one needs to increase the network connectivity as much as possible while on the other hand, the experimental measurements indicate that we need to limit the number of concurrent transmitters for better reception ratio of the capture effect. Combining those two results, we can see the key for a faster convergence of SBGP is therefore to increase the network connectivity while concurrently keeping a low probability of interference. Simply increasing the transmission range of the node to reach far away node will also increase the expected number of concurrent transmissions and hence interference at the receiver. Previously mentioned multi-channel approaches may decrease the probability of collisions but is helpless in increasing the network connectivity.

We take a different approach to solve the aforementioned issues, which is to utilize the emerging multi-radio sensor nodes. Unlike the aforementioned multi-channel approaches with a single radio which has homogeneous characteristics for each channel, the multiple heterogeneous radios can provide various transmission range, frequency, data rate and power efficiency, which are capable of increasing the network connectivity without increasing the probability of interference to the capture effect in large and dense networks. The resulting system, according to our performance analysis result, should provide significant performance improvements in large scale networks. Hence, in this paper, we will investigate the ways to adopt the multi-radio approach into SBGP and fully utilize its potential to reduce the interference and accelerate information disseminations in SBGP.

4.1 Clustering

Intuitively, to fully utilize the capability of multiple radio with different transmission range capabilities, the network can be divided into clusters based on the location of the nodes. Depending on the number of radios equipped in the sensor nodes, the entire sensor network can be organized into a hierarchical structure of multiple levels of clusters, or cluster trees as shown in 4. For each level, a single radio handles communications within that level, i.e., low-power radio for short range communications and high-power radio

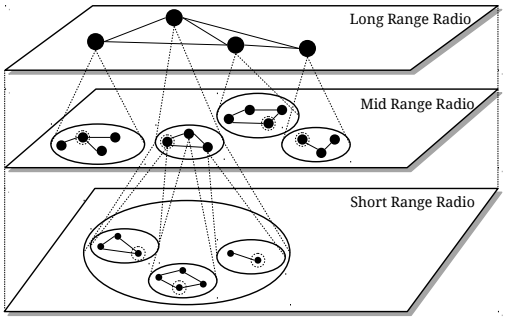

Figure 4: Cluster Tree Multi-Radio Communication

for long range communications, minimizing the interference within and between clusters and therefore improving the scalability of the all-to-all communications.

There are many existing work on clustering algorithms in wireless sensor networks [4, 5, 8, 11, 15] and the studies of clustering algorithms are out of the scope of this paper. Here we assume that a distributed clustering algorithm has been implemented in the target wireless sensor networks. We also assume that after being clustered, each node will have its unique ID within the cluster and will be made aware of the node ID of its cluster head and the size of the cluster. Additionally, each cluster head will also be assigned with a cluster ID and be aware of the total number of clusters. Currently, two heterogeneous radios are equipped in commonly available sensor nodes - one in 2.4GHz for short range communication and the other in sub-GHz (868/915MHz) for mid to long range communication. Taking the advantages of both radios, the network can therefore be divided into two levels. By running the clustering algorithm during the initialization, the network will be divided geographically into several clusters of similar sizes and one node inside each cluster will be chosen to become the *cluster head*.

4.2 Communication Protocols

After clustering, the network communications are now comprised of intra-cluster communications with short-range radio and inter-cluster communications through the cluster heads with long range radio. Similar to the Chaos system [16], our approach will use a bitmap flags field to help aggregating data instead of simply mixing of data. We will discuss the communication protocols used at each level and temporal ordering between them in the following.

4.2.1 Inter-cluster Communication. Cluster heads exchange information with each other through inter-cluster communication, which will be done using the long-range radio since the network is geographically clustered and the distance between cluster heads is presumably greater. Each cluster head will run the SBGP to communicate with each other, with the assumption that the long-range radio is powerful enough to make the sub-network between the cluster heads fully-connected.

4.2.2 Intra-cluster Communication. Nodes inside a cluster exchange information with other cluster members and the cluster head through intra-cluster communication. Since the nodes are geographically clustered together, low-power short-range radio will be used in intra-cluster communication to reduce energy consumption and interference with nodes in other clusters.

With the short-range radio, it is still possible that nodes in one cluster are interfered or overheard by nodes from adjacent clusters. Such overhearing certainly helps the dissemination of information and reduces latency. However, to support overhearing from nodes in nearby clusters, a flags field of a significantly larger size would be required in the packet to record every node in the entire network, easily exceeding the frame size of 802.15.4 and hurting the scalability of the system. Hence in our multi-radio approach, we choose to ignore such overhearing and nodes will use a flag field that is specific to its cluster, which can have a much smaller size.

Depending on the size of the clusters established by different clustering algorithms and the transmission range of the short-range radio, two schemes may be used for intra-cluster communication: *Many-to-one* scheme using unicast and TDMA-based protocols, and *Many-to-many* scheme using SBGP, as shown below:

- *Many-to-one* protocol. When all the cluster members are with in the communication range of the cluster head, a TDMA scheduling-based transmission can be maintained by the cluster head so that each of its cluster members is able to send its packets directly to the cluster head one by one. Considering the short range of the radio, the size of such cluster will also be low, which means less overhead in TDMA coordination and potentially good performance.
- *Many-to-many* protocol. When the cluster size increases and a node requires multi-hop communication through the short-range radio to reach the cluster head, the TDMA-based many-to-one communication becomes less efficient and less reliable. In such case, we will use the SBGP protocols which have been proven to be reliable in dynamic environment and does not require coordination between nodes. This approach will have a significant advantage on the latency however the nodes are required to stay awake during the entire process.

4.2.3 Temporal Ordering. Based on the sensor nodes' capability of operating multiple radios at the same time, the intra-cluster and inter-cluster communication can be done either a) simultaneously until the entire network converges, or b) sequentially in the following three phases,

(a) Each cluster will first do intra-cluster communications to let the cluster head collect all the information within its cluster using either many-to-one scheme or many-to-many scheme.
(b) Only after the cluster head completes the collection, the inter-cluster communication will start, where cluster heads exchange their aggregated information of their own clusters using the many-to-many Chaos scheme.
(c) Once the cluster head has collected all the information from other clusters, it will initiate a flooding-based (e.g. [21]) intra-cluster communication or simply broadcasting to its one-hop cluster members in order to disseminate the aggregated information to all its cluster members and the entire network will then reach convergence.

Both schemes have their advantages and disadvantages in terms of latency and energy consumption. For simultaneous intra and

inter-cluster communications, the latency of both phase can be overlapped, leading to a lower overall convergence latency. However, the number of transmissions will increase, especially for long-range radio, resulting in a higher energy consumption. The sequential communication scheme, on the other hand, saves energy since the cluster head uses long-range radio only after it collects all the information from its cluster and each transmission through long-range radio contains more information compared with simultaneous scheme. Therefore, cluster heads will quickly converge using less expensive long-range radio transmissions. The sequential scheme however, will result in higher latency, especially when the cluster size is comparable to the number of clusters.

In summary, the four scheme utilizing multi-radio are shown in Table 2 below. In Section 5, all these scheme will be evaluated and compared in various experimental configurations.

Table 2: Communication schemes with Multiple Radios

	Many-to-many	Many-to-one
Sequential	Scheme 1	Scheme 2
Simultaneous	Scheme 3	Scheme 4

5 EVALUATION

In this section, we will evaluate the proposed the system. The performance of the aforementioned four schemes of multi-radio hierarchical system and the original SBGP system will be evaluated and compared under various experiment settings including network size and network density.

5.1 Setup

To evaluate the proposed approach, we have implemented all four multi-radio schemes and the single radio SBGP protocol (which is also used in the previous validation in Section 3) in MASON simulator toolkit [19]. The MASON toolkit is an open source multi-agent simulation system written in Java. Though MASON is commonly used in swarm robotics and computational social science studies, it is also suitable to model the wireless sensor networks as each sensor node can be easily modeled as an individual *agent* and the communications are done through the interactions between agents.

In the simulation, we assume the sensors are all perfectly synchronized. In each round, all the node will randomly choose whether to broadcast or receive. For simplicity, the radio propagation models are not considered in the simulation. Instead, two node will be able to communicate if the distance between them is less than the radio communication range. Subsequently, the capture effect is empirically modeled based on the experimental result in [16]. Specifically, when there are multiple concurrent transmitters within the neighborhood of a node, the probability of that node receiving from any one of the transmitters is equal.

The network topology in the simulation is based the *Geometric Random Graph* where the nodes are randomly placed in a squared 2-D space. The range of the short-range radio is set in a way that the network is connected and the average number of neighbors satisfies the given value. The range of the long-range radio is set so that all the cluster heads forms a fully connected network. The clustering of the network is done statically and manually in a grid-like fashion in order to precisely control the cluster size and number of clusters. The initial cluster head will be randomly selected in each cluster.

5.2 Result

We have simulated the four multi-radio schemes and the single radio SBGP system with 100 to 100000 nodes and average degrees of the nodes in the network: 5, 25, and 50. Also, to enable the many-to-one schemes, we set the cluster size to be the same with the degree. For each setting, 10 independent runs with different random number generator seeds are conducted. We focus our performance metrics on the convergence latency.

Figure 5 show the convergence latency of the four multi-radio schemes (namely MR-Scheme 1, 2, 3, and 4) and the original single radio SBGP protocol (SR) under different network size and density. The x-axis represents the size of the network (number of the nodes) in logarithmic scale. The y-axis represents the convergence latency in time slots. As we can see from the figure, first all four multi-radio schemes outperform the single radio protocol at all three density levels and all four node sizes as expected, indicating that multi-radio approach is able to increase the network connectivity and at the same time maintaining a low chance of interference. The highest improvement — 42% reduction in convergence latency, is achieved by MR-Scheme 3 when $N = 10^5$ and $d = 50$. Also as we can see in Figure 5(b), the latency of the single radio SBGP protocol is the lowest, indicating a better-balanced case between the interference from concurrent transmissions and the network connectivities.

Among the four schemes, we can see that at lower density level which also means small cluster size, the MR-Scheme 2 and MR-Scheme 4 which uses many-to-one protocols for intra-cluster communications outperforms the the other two scheme, indicating an good performance of the TDMA-based many-to-one protocol in small size clusters compared with the SBGP. When the number of nodes increases, since the cluster size is constant, the number of clusters keeps increasing. This means the number of cluster heads that are concurrent transmitting also increases, reducing the efficiency of the inter-cluster communication and causing the all four schemes to lose much of its performance advantage over the single-radio protocol. When it comes to higher network density and larger cluster size, TDMA-based protocol starts to become less efficient compared with the SBGP protocols for the intra-cluster communications. As a result, we can learn from Figure 5(c) that MR-Scheme 2 and 4 performs significantly worse than MR-Scheme 1 and 3 when the network size is relatively small. Also with a larger cluster size, the performance of the MR schemes in Figure 5(c) at larger network size gained significant improvements compared with that in Figure 5(a) due to a decreased number of concurrent cluster heads participating in the inter-cluster communication and therefore improved capture effect reception ratio. In contrast, with higher density, the single radio SBGP suffers more from interference and the performance is the worst among all three densities.

Between the sequential and simultaneous schemes, as we can see from the result, the latency difference is not very significant. Since the simultaneous schemes frequently activates its long-range radio, such result indicates a trade-off that the sequential schemes is more suitable without slowing down too much in cases where the energy consumption is a major concern for network operation.

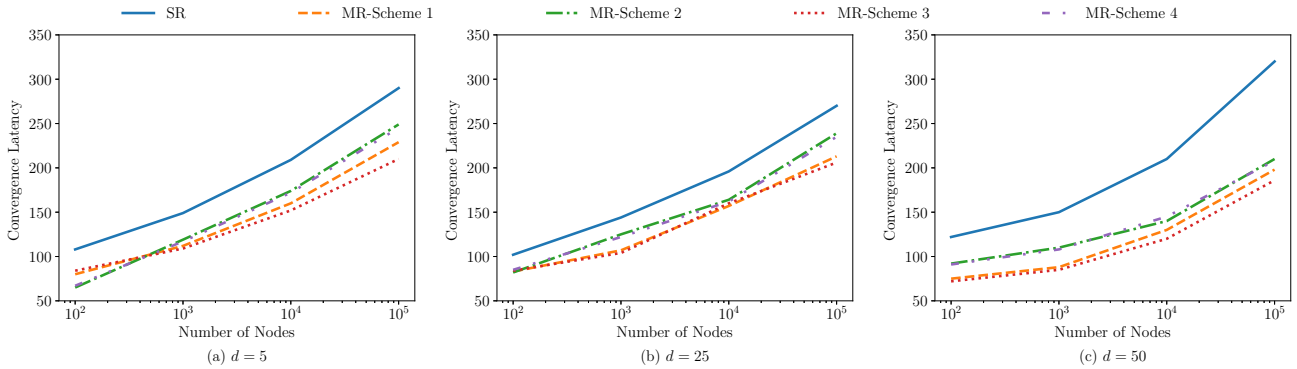

Figure 5: Convergence latency vs. Network size in various node degree (a) $d = 5$, (b) $d = 25$, (c) $d = 50$

6 CONCLUSION

In this paper, we studied the performance of the synchronous broadcasting gossip-based protocols. We first investigated the performance of SBGP through theoretical modeling and mean analysis. We have derived exact bound of the convergence latency for complete graphs and approximations for other types of topologies. We have validated the theoretical result based on the numerical result and simulations. Based on the theoretical result from the performance model, we proposed a multi-radio approach to improve the performance of the SBGP protocols in large and dense networks. We have investigated the performance of four multi-radio schemes through simulations. Result has shown that the multi-radio approach can reduce the convergence latency up to 42%.

ACKNOWLEDGMENT

This work is supported by US National Science Foundation under grant CI-EN 1727303.

REFERENCES

[1] Beshr Al Nahas, Simon Duquennoy, and Olaf Landsiedel. 2017. Network-wide Consensus Utilizing the Capture Effect in Low-power Wireless Networks. In *Proceedings of the International Conference on Embedded Networked Sensor Systems (ACM SenSys 2017)*. 14.

[2] Beshr Al Nahas and Olaf Landsiedel. 2016. Competition: Towards Low-Latency, Low-Power Wireless Networking under Interference.. In *EWSN*. 287–288.

[3] Tuncer C Aysal, Mehmet E Yildiz, Anand D Sarwate, and Anna Scaglione. 2009. Broadcast gossip algorithms for consensus. *Signal Processing, IEEE Transactions on* 57, 7 (2009), 2748–2761.

[4] Seema Bandyopadhyay and Edward J Coyle. 2003. An energy efficient hierarchical clustering algorithm for wireless sensor networks. In *INFOCOM 2003. Twenty-Second Annual Joint Conference of the IEEE Computer and Communications. IEEE Societies*, Vol. 3. IEEE, 1713–1723.

[5] Suman Banerjee and Samir Khuller. 2001. A clustering scheme for hierarchical control in multi-hop wireless networks. In *INFOCOM 2001. Twentieth annual joint conference of the IEEE computer and communications societies. Proceedings. IEEE*, Vol. 2. IEEE, 1028–1037.

[6] Florence Benezit, Patrick Denantes, Alexandros G Dimakis, Patrick Thiran, and Martin Vetterli. 2008. Reaching consensus about gossip: convergence times and costs. *Information Theory and Applications* (2008).

[7] Stephen Boyd, Arpita Ghosh, Balaji Prabhakar, and Devavrat Shah. 2006. Randomized gossip algorithms. *IEEE transactions on information theory* 52, 6 (2006), 2508–2530.

[8] Haowen Chan and Adrian Perrig. 2004. ACE: An emergent algorithm for highly uniform cluster formation. In *European workshop on wireless sensor networks*. Springer, 154–171.

[9] Bogdan S Chlebus and Dariusz R Kowalski. 2002. Gossiping to reach consensus. In *Proceedings of the fourteenth annual ACM symposium on Parallel algorithms and architectures*. ACM, 220–229.

[10] Dimitrios Chronopoulos. 2016. *Extreme Chaos: Flexible and Efficient All-to-All Data Aggregation for Wireless Sensor Networks*. Master's thesis. Delft University of Technology.

[11] Murat Demirbas, Anish Arora, and Vineet Mittal. 2004. FLOC: A fast local clustering service for wireless sensor networks. In *Workshop on Dependability Issues in Wireless Ad Hoc Networks and Sensor Networks (DIWANS/DSN 2004)*. 1–6.

[12] Fabio Fagnani and Sandro Zampieri. 2008. Asymmetric randomized gossip algorithms for consensus. *IFAC Proceedings Volumes* 41, 2 (2008), 9051–9056.

[13] Fabio Fagnani and Sandro Zampieri. 2008. Randomized consensus algorithms over large scale networks. *IEEE Journal on Selected Areas in Communications* 26, 4 (2008).

[14] Miroslav Fiedler. 1973. Algebraic connectivity of graphs. *Czechoslovak mathematical journal* 23, 2 (1973), 298–305.

[15] Wendi B Heinzelman, Anantha P Chandrakasan, and Hari Balakrishnan. 2002. An application-specific protocol architecture for wireless microsensor networks. *IEEE Transactions on wireless communications* 1, 4 (2002), 660–670.

[16] Olaf Landsiedel, Federico Ferrari, and Marco Zimmerling. 2013. Chaos: Versatile and efficient all-to-all data sharing and in-network processing at scale. In *Proceedings of the 11th ACM Conference on Embedded Networked Sensor Systems*. ACM, 1.

[17] A. Laradji and A. Umar. 2006. Combinatorial Results for Semigroups of Order-PreservingFull Transformations. *Semigroup Forum* 72, 1 (01 Feb 2006), 51–62. https://doi.org/10.1007/s00233-005-0553-6

[18] Jiakang Lu and Kamin Whitehouse. 2009. *Flash flooding: Exploiting the capture effect for rapid flooding in wireless sensor networks*. IEEE.

[19] Sean Luke, Robert Simon, Andrew Crooks, Haoliang Wang, Ermo Wei, David Freelan, Carmine Spagnuolo, Vittorio Scarano, Gennaro Cordasco, and Claudio Cioffi-Revilla. 2018. The MASON Simulation Toolkit: Past, Present, and Future. In *International Workshop on Multi-Agent Systems and Agent-Based Simulation*. Springer, 51–62.

[20] Tomasz Pazurkiewicz, Michal Gregorczyk, and Konrad Iwanicki. 2014. NarrowCast: A New Link-Layer Primitive for Gossip-Based Sensornet Protocols. In *Wireless Sensor Networks*, Bhaskar Krishnamachari, Amy L. Murphy, and Niki Trigoni (Eds.). Springer International Publishing, Cham, 1–16.

[21] James Pope and Robert Simon. 2015. Efficient one-to-many broadcasting for resource-constrained wireless networks. In *Local Computer Networks (LCN), 2015 IEEE 40th Conference on*. IEEE, 518–525.

[22] Coen Roest. 2015. *Enabling the Chaos Networking Primitive on Bluetooth LE*. Master's thesis. Delft University of Technology.

[23] N. J. A. Sloane. 2007. The On-Line Encyclopedia of Integer Sequences. http://oeis.org/A000248 Sequence A000248: Number of forests with n nodes and height at most 1.

[24] N. J. A. Sloane. 2015. The On-Line Encyclopedia of Integer Sequences. http://oeis.org/A259760 Sequence A259760: Triangle read by rows: T(n,k) is the number of partial idempotent mappings (of an n-chain) with breadth exactly k.

[25] N. J. A. Sloane. 2017. The On-Line Encyclopedia of Integer Sequences. http://oeis.org/A286910 Sequence A286910: Number of independent vertex sets in the n-antiprism graph.

[26] F. Wang, M. T. Thai, Y. Li, X. Cheng, and D. Z. Du. 2008. Fault-Tolerant Topology Control for All-to-One and One-to-All Communication in Wireless Networks. *IEEE Transactions on Mobile Computing* 7, 3 (March 2008), 322–331. https://doi.org/10.1109/TMC.2007.70743

[27] Haoliang Wang and Robert Simon. 2016. Modelling wireless sensor networks with energy harvesting: A stochastic calculus approach. In *Modeling and Optimization in Mobile, Ad Hoc, and Wireless Networks (WiOpt), 2016 14th International Symposium on*. IEEE, 1–8.